Astron. Astrophys. 325, 277–281 (1997)

ASTRONOMY AND ASTROPHYSICS

Spectroscopy of the protoplanetary nebula AFGL 618

M. Baessgen[1], **W. Hopfensitz**[1], **and J. Zweigle**[2]

[1] Institut für Astronomie und Astrophysik, Abteilung Astronomie, Universität Tübingen, Waldhäuserstr. 64, D-72076 Tübingen, Germany
[2] Institut de Radio Astronomie Millimétrique (IRAM), 300 Rue de la Piscine, F-38406 Saint Martin d'Héres, France

Recieved 30 September 1996 / Accepted 16 January 1997

Abstract. We report on new optical spectroscopic observations of the protoplanetary nebula AFGL 618. Compared to older observations we find a change in some emission line ratios indicating dynamical evolutionary processes during the last few years. Possible reasons for this behaviour are discussed.

Key words: planetary nebulae: AFGL 618 – stars: AGB – post: AGB

1. Introduction

The first spectra in the visual and infrared range of the protoplanetary nebula AFGL 618 were taken by Westbrook et al. (1975). They found, that AFGL 618 is a bright infrared object associated with a pair of small visual nebulosities each of which has a diameter of 2 to 3 arcsec and that the large linear polarization exhibited at visible wavelengths is a strong indication of reflection nebulosity. The eastern component is 3 to 4 times brighter than the Western component and the observed Balmer decrements indicates a substantial, but identical, reddening of A_v = 3.5 to these two lobes. The compact HII region in the center, obscured by dust, is in a transition evolutionary stage in which an ionization front expands rapidly into the surrounding medium (Kwok and Bignell 1984). Schmidt and Cohen (1981) (SC81) argued from their spectropolarimetric studies, that the forbidden line emission arises within the nebulous lobes themselves and becomes polarized upon transmission through the intervening galactic medium. They calculated that most of the visible emission by permitted lines originates, very near the star and is scattered in the observers direction by grains in the lobes. It is likely that an additional portion of the permitted line radiation is emitted within the lobes themselves, and should be polarized like the forbidden lines. They describe the lobes of AFGL 618 by a simple two component model, consisting of a neutral and an ionized component associating them with shadowed and unshadowed material, respectively. Goodrich (1991) stress the fact that the optical spectrum of the east lobe of AFGL 618 is similiar to spectra of Herbig-Haro objects. Carsenty and Solf (1982) (CS82) found by investigation of the kinematical structure of the bipolar nebula, that the radial velocity difference of the centroids of the lobes is 114 kms^{-1} in the forbidden lines but only 68 kms^{-1} in the Balmer lines. The velocity extent of the hydrogen lines is similar to that of the forbidden lines. This shows that these lines are emitted not only in the central region but also in the blobs. Cernicharo et al. (1989) have reported the detection of a massive outflow with velocities of 2OO kms^{-1} in the lines of CO, HCN, HC3N and HCO+. This outflow was studied in detail by means of interferometric observations of HCN by Neri et al. (1992). Among the many other publications of the object the work of Kelly, Latter and Rieke (1992) (KLR92) is from special interest for us because it offers the possibility to compare their emission line fluxes with ours in order to study evolutionary effects. They present for both lobes an extensive list of emission line fluxes. Using diagnostic lines they showed, that there is both high- and low-temperature gas in the lobes. Trammell, Dinerstein and Goodrich (1993) (TDG93) report about spectropolarimetric observations of AFGL 618. They were able to separate the emission line fluxes into a scattered part originating in the central region and an unscattered part which is emitted in the blobs. In the following we present spectroscopic observations of both in the wavelength region between 370 nm and 800 nm. The observational parameters are described in Sect. 2 and in Sect. 3 we discuss our results.

2. Observations

The spectroscopic observations of AFGL 618 were done on October 29, 1994 with the twin-spectrograph of the 3.5m DSAZ (Deutsch Spanisches Astronomie Zentrum) telescope on Calar Alto (Spain) in photometric conditions. The linear dispersions of the gratings used in the blue and red channel of the spectrograph were 3.6 nmmm^{-1}, that corresponds to 0.086 nm pixel^{-1} on the CCD-chips (1024 $\times$ 1024 pixel of size 24μm $\times$24μm) installed in the spectrograph. The twin-spectrograph simultaneously takes two spectra in the blue and red wavelength range, each of them covering about 80 nm. So we needed three red and three blue spectra to obtain a total spectrum from about 370 nm to 800 nm with some overlap between the spectra. The exposure

Send offprint requests to: M. Baessgen

Table 1. Uncorrected and dereddened emission line fluxes for the bright and the faint lobe, normalized to $H\beta$ = 100, velocity differences and spatial separations between the two lobes, measured for different emission lines

Line	Br. lobe (uncorr.)	Br. lobe (dered.)	F. lobe (uncorr.)	F. lobe (dered.)	v-Diff. [kms^{-1}]	Sep. [$''$]
H8 388.9, HeI 388.9	7.6	18.4				
[FeII] 393.1, 393.4	4.5	10.5				
Hε 397.0	12.4	27.7				
[SII] 406.7	30.9	62	56	108.9	111	8.2
[SII] 407.4	10.9	21.7	17	33.9	110	8
Hδ 410.1	17.3	33.8	15.4	30.2	51	7.3
[FeII] 424.4, [FeII] 424.5	2	3.7				
[FeII] 427.7	0.8	1.5				
[FeII] 428.7	1.6	2.8				
Hγ 434.0	33.1	55.8	33	53.8	35	7.5
[FeII] 441.4-441.6	3.1	4.8				
[FeII] 447.0, HeI 447.1	3.2	4.7				
MgI 457.1	8.9	11.9	19	25.5	92	8.2
[FeII] 464.0	2.6	3.3				
λ 456.1	4.8	6.5				
FeII 465.7, [FEIII] 465.8	6.4	8.6				
[FeIII] 470.1	3.1	3.7				
[FeIII] 481.4	1.3	1.4				
Hβ 486.0	100	100	100	100	49	7.5
[FeII] 500.6, 500.7, [OIII] 500.7	4.9	4.4	6.2:	5.5:	102	8.2
[FeII] 515.8, 515.9	6.1	4.8	11	8.7	122	8.4
[NI] 520.0	89	68.2	148	113	121	7.5
[FeII] 526.0	2.7	1.5				
[FeIII] 526.9	9.1	4.9				
[FeII] 533.4	1.9	1.3				
[FeII] 537.7	1.8:	1.2:				
[FeII] 541.3	1.8	1.2				
[FeII] 552.7	2.8:	1.6:				
[OI] 557.7	3.4	1.8				
[NII] 575.5	22.9	10.9	27	12.4	47	7.2
HeI 587.6	13.3	5.9				
NaI 589.0	3:	1.3:				
NaI 589.6	1.7:	0.7:				
[OI] 630.0	420	137	1240	404	95	7.9
[SIII] 631.2	9.1	2.9	2.5	0.8	14:	6.4
[OI] 636.3	141	45	424	134	94	7.8
[NII] 654.8	53	15.6	83	24.2	101	7.8
Hα 656.3	970	281	1076	312	41	6.9
[NII] 658.3	17	49	258	74	100	7.9
HeI 667.8	5.7	1.5				
[SII] 671.7	121	32	253	67	107	7.5
[SII] 673.1	220	57.8	489	128	103	7.5
λ 700.0	1.4	0.3				
HeI 706.5	12.1	2.8	15	3.4	30	6.3
[ArIII] 713.5	8.7	2				
λ 715.2	18.8	4.1	54	11.7	109	8.3
[FeI] 716.8	4.7	1	5.3	1.1	109	7.5
[FeI] 729.0, [CaII] 729.1	31.6	6.6	88	18.3	99	8.7
[OII] 732.0	108	22.1	134	27.6	20	6.7
[OII] 733.0	74.3	15.2	67.9	13.9	61	6.4
[FeII] 737.1	13.1	2.6	30.7	6	106	8
[FeI] 740.7	2.5	0.5				
[FeII] 744.9	7	1.4	18.6	3.7	105	7

Table 1. (continued)

Line	Br. lobe (uncorr.)	Br. lobe (dered.)	F. lobe (uncorr.)	F. lobe (dered.)	v-Diff. [kms^{-1}]	Sep. [$''$]
[FeII] 763.7	1.4	0.3	93	17.2	153	7.5
[FeII] 768.6-768.8	2.3	0.4				
λ 779.0	2.4	0.5				
λ 783.7	3.1	0.6				
[FeI] 795.9	2	0.4				
[FeII] 799.9	3.7	0.7				

times for all spectra were 20 minutes. The slit length was $4'$, the slit width was chosen to $1.2''$ and its orientation was east-west covering both lobes of the object. Along the slit each pixel is $0.89''$ in both channels. We used standard MIDAS procedures to reduce the data. To correct for the wavelength dependency of the gratings and CCDs, spectra of standard stars were taken.

3. Results and Discussion

3.1. Extinction

The determination of the extinction of the object is a quite difficult problem. Because of the dust obscuring the object there may be a lot of internal absorption eventually different for both lobes. An additional difficulty is that some of the lines are seen as scattered light. Some authors of other works try to determine A_v separately for both lobes. TDG93 determined a different extinction for the scattered and unscatterd spectra for the eastern and western lobe. They found a large amount of internal extinction in the eastern lobe but not in the Western lobe. They measured for the total flux a much bigger Hα/Hβ-ratio in the eastern than in the Western lobe. In our measurements we found nearly the same Hα/Hβ-ratio in both lobes. So we decided for sake of simplicity and the better possibility of comparison our work with others, to adopt only one extinction coefficient of $E(B-V) = 1.1$ for both lobes. This value was determined using the Hα/Hβ-ratio and the extinction law of Seaton (1979). Because this is a rather crude procedure we have to use some care to interprete the results.

3.2. The emission line fluxes

Because our slitwidth was smaller than the diameter of the blobs we only obtained relative line fluxes, i.e. we normalized all lines to Hβ = 100. Table 1 shows uncorrected and dereddened line fluxes for both lobes.

3.3. Spectral and spatial resolution of the spectra

The dispersion of the spectra is about 35..50 kms^{-1} per pixel but fitting the emission lines using gaussian profues we are able to determine the centroids of the lines to about 10 kms^{-1}. Table 1 lists these obtained velocity differences between faint and bright lobe.

We find two groups of lines, the forbidden lines with a difference of the line centroids of 100 ± 129 kms^{-1} and the permitted recombination lines with a velocity difference of 41 ± 18 kms^{-1}. These results are in good agreement with CS82. The only exception are the [OII] 732.0 nm, [OII] 733.0 nm, [NII] 575.5 nm and [SIII] 631.2 nm lines which show small velocity differences. Fig. 1 shows the wavelength region around 575.5 nm. As comparison the spectrum around the strong [NII] lines and Hα is shown in Fig. 2. We will discuss this result later.

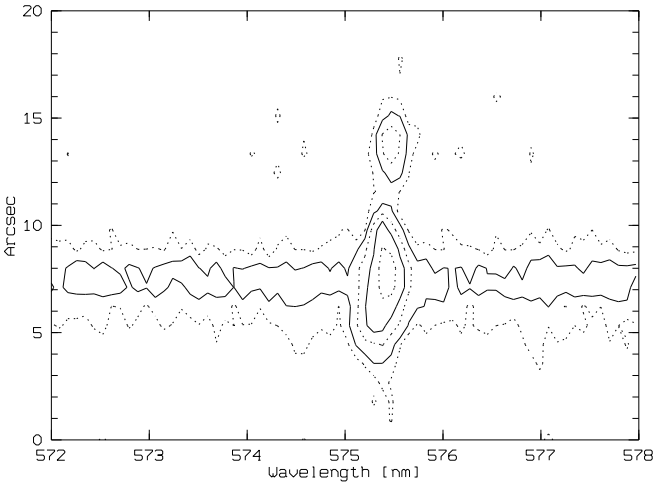

Fig. 1. Cut from the twodimensional longslit spectrum around the [NII] line at 575.5 nm

Next we determined the spatial positions of the emission line maxima and measured the separation between the two lobes. The distance differences are very small of course and should be treated with some caution but nevertheless we believe that they show some interesting results. Table 1 also shows these spatial separations.

Again we find two groups but not so well separated as the velocity difrerence of the permitted and forbidden lines. One group mainly contains the recombination lines while most forbidden lines are in the other group. This is shown in Fig. 3. A very interesting result is that the same four forbidden lines which are in the 'wrong' velocity-difference-group are also in the the 'wrong' spatial-difference-group.

If the model is correct that the recombination lines are mainly scattered by the lobes, we would expect the peak emission at the inner edges of the lobes while the forbidden lines are emitted in the whole blobs showing their peak intensities a little more separated. Fig. 4 shows this in a simple diagram.

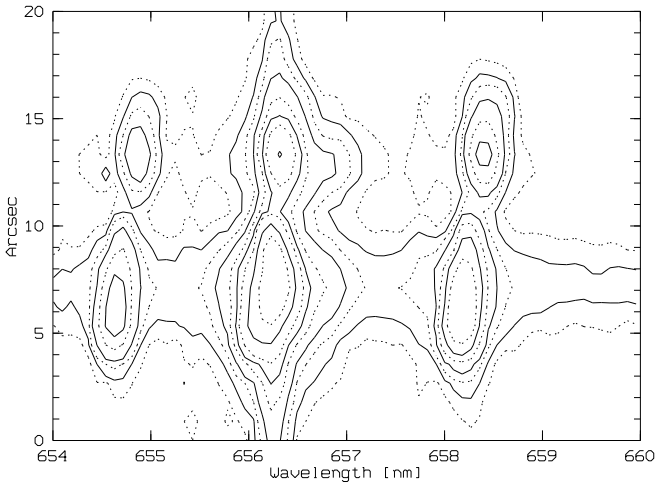

Fig. 2. Cut from the twodimensional longslit spectrum around the Hα line at 656.3 nm

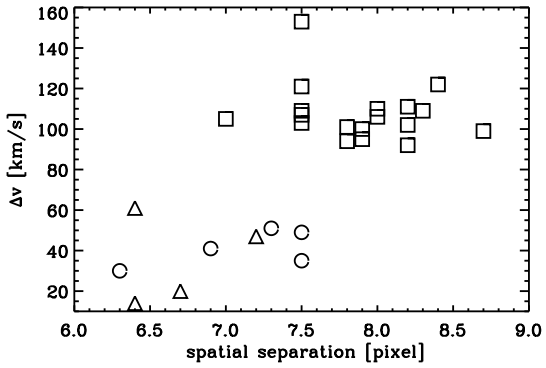

Fig. 3. Spatial and velocity difference between eastern and west blob, circles are recombination lines, triangles are forbidden lines w a critical density bigger than 10^6 cm^{-3} and rectangles are forbid lines with critical density smaller than 10^6cm^{-3}

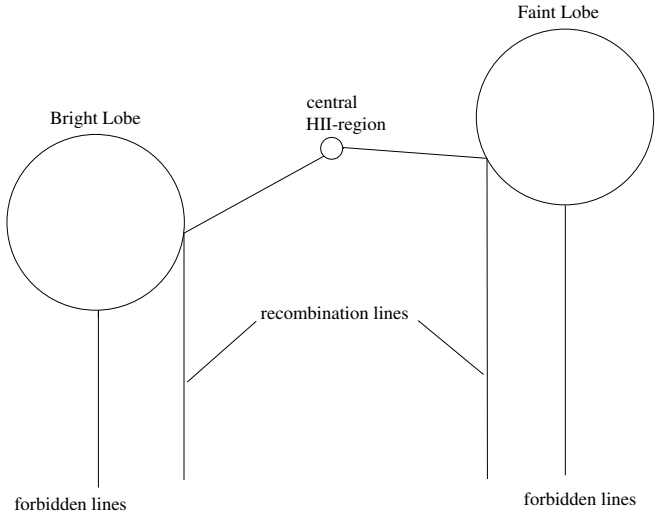

Fig. 4. Simple geometrical model of AFGL 618, the observer's position is at the bottom, the dashed lines show the paths of the scattered photons originating from the central HII-region, the full lines those of the photons emitted in the blobs.

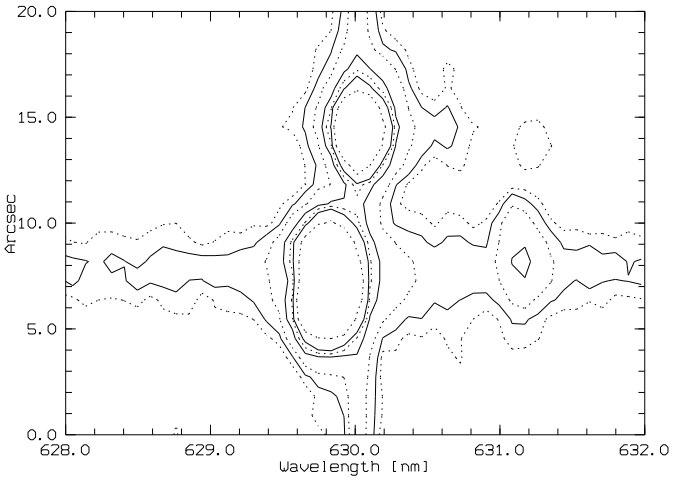

Fig. 5. Cut from the twodimensional longslit spectrum around the [SIII] line at 631.2 nm

What remains is to explain why there are 'exceptions', especially why seem different [NII] lines to be emitted in different regions?

3.4. The [NII]-lines

We compared the strengths of the [NII] lines 654.8 nm, 658.3 nm and 575.5 nm with previous publications. The measurement of SC81 were done in 1979, those of KLR92 in 1989 and ours in 1994. KLR92 give line strength values uncorrected for extinction, SC81 give dereddened fluxes for an adopted extinction of A_v = 3.5. We corrected our fluxes and those of KLR92 with $E(B-V)$ = 1.1 and recalculated the values of SC81 also with $E(B-V)$ = 1.1 to be able to make an extinction independent comparison of the different observations. Table 2 shows the obtained [NII](654.8+658.3) /[NII](575.5) ratios. Between the KLR92 and the SC81 observations the [NII] line ratio significantly changed in the bright lobe but not in the faint lobe. The authors argued that a shock had reached the bright lobe producing rapid heating and ionization. Now, some years later we observe a similar phenomenon in the faint lobe. Because the strength of the [NII] 575.5 nm line is more temperature dependent than the [NII] 654.8 nm and the [NII] 658.3 nm lines, the regions of the strongest [NII] 575.5 nm emission are moving towards the inner edges of the blobs where the shock hits the blobs which is consistent with our observations. Since the critical density of the 575.5 nm line is very high ($\approx 10^8$cm^{-3}) this line is also emitted in the central region of AFGL 618 as shown by TDG93. The scattered emission in the [NII] 575.5 nm line is about 42% in the eastern lobe and less than 40% in the western lobe (TDG93). But only about 15% of the [NII] emission line flux at 654.8 nm and 658.3 nm is scattered in the eastern lobe and 8% in the western lobe, respectively. This also explains

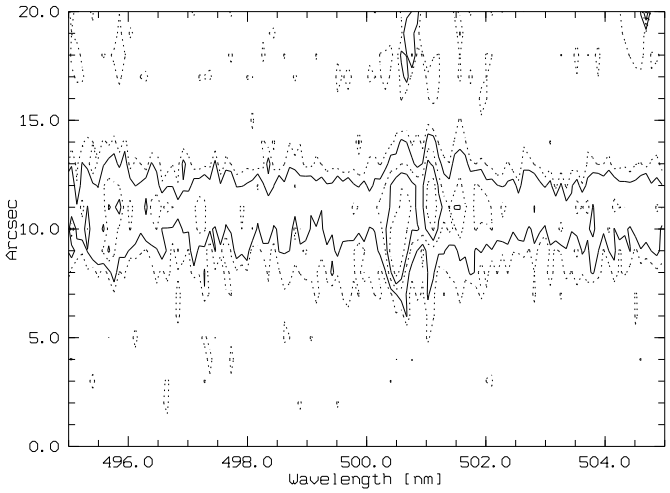

Fig. 6. Cut from the twodimensional longslit spectrum around 500.7 nm

the relatively small velocity separation. Since an appreciable amount of the [NII] 575.5 nm emission originates from the central HII-region which is expanding slower than the lobes. The critical densities of the [OII] lines at 732 nm and 733 nm are also relatively high ($\approx 10^7$ cm^{-3}) and are emitted in the central region and in the blobs. So it is still not quite clear what really happened. Did due to shocks the temperature in the blobs increase? Or did the density of the central region decrease below the critical density of the [NII] 575.5 nm line (about 10^8 cm^{-3}), so that we see scattered light of this line? We have no continuous spectroscopic observations of the object so we do not know whether the increase of the [NII] 575.5 nm line was a rather fast or a slow process. If there are shocks leading to a temperature enhancement in the lobes some lines of higher ionized atoms should also be visible.

3.5. Emission lines of double ionized ions

We find some weak but clearly visible emission lines of double ionized ions in the bright lobe. In the faint lobe we can only see some weak indications of these lines. These lines are the [ArIII] 713.5 nm line (ionization potential (IP) 27.6 eV) and the [SIII] 631.2 nm line (IP 27.3 eV). [SIII] lines at 906.9 nm and 953.1 nm were already seen by KLR92. There are also lines of [FEIII] but the IP is only 16.2 eV. Fig. 5 shows the twodimensional spectrum around the [SIII] 631.2 nm line and Fig. 6 shows the wavelength region around 500.7 nm. Since in this region are some [FEII] lines no definitive identification of [OIII] can be done.

Table 2. [NII](654.8+658.3)/[NII](575.5) ratio dereddened with $E(B-V)$ = 1.1 from different observations made by different authors

	Br. lobe	F. lobe
SC81	16.1	13.0
KLR92	7.8	16.7
this work	5.9	7.6

4. Conclusion

The protoplanetary nebula AFGL 618 is one of the few objects in this transition stage where dynamical processes were directly observed over the last twenty years. Observations with better spectral and spatial resolution at least in some wavelength ranges should be done to investigate the exact velocity distribution inside the object in more detail. Furthermore new spectropolarimetric observations would give the possibility to distinguish between emission from the central HII-region and the lobes. Then it should be possible to construct a spatio-kinematical model which consistently describes the spectroscopic observations.

References

Carsenty, U., Solf, J., 1982, A&A 106, 307
Cernicharo, J., Guelin, M., Martin-Pintado, J., Penalver, J., Mauersberger, R., 1989, A&A 222, L1
Goodrich, R.W., 1991, ApJ 376, 654
Kwok, S., Bignell R.C., 1984, ApJ 276, 544
Kelly, D.M., Latter, W.B., Rieke, G.H., 1992, ApJ 395, 174
Neri, R., Garcia-Burillo, S., Guelin, M. et al., 1992, A&A 262, 544
Schmidt, G.D., Cohen, M., 1981, ApJ 246, 444
Seaton, M.J., 1979, MNRAS 187, P73
Trammell, S.R., Dinerstein, H.L., Goodrich, R.W., 1993, ApJ 402, 249
Westbrook, W.B., Becklin, E.E., Merrill, K.M. et al., 1975, ApJ 202, 407

This article was processed by the author using Springer-Verlag LaTeX A&A style file *L-AA* version 3.